19th Brazilian Congress of Thermal Sciences and Engineering
November 06th-10th, 2022, Bento Gonçalves - RS - Brazil

ENC-2022-0366
STUDY OF FLAME ACCELERATION IN A CLOSED DUCT USING EFFECTIVE LEWIS AND ZELDOVICH NUMBERS AS PARAMETERS

Guilherme Rodrigues Cardoso
Carlos Henrique Lauermann
Rafael Quines da Silva
Manuel António Kiony Nzinga
Thamy Cristina Hayashi
Andrés Armando Mendiburu Zevallos
Universidade Federal do Rio Grande do Sul, Departamento de Engenharia Mecânica - Rua Sarmento Leite, 425 - Centro Histórico, Porto Alegre - RS, 90050-170
cardosogui.1@hotmail.com
carlos.lauermann@ufrgs.br
rafael.quines@ufrgs.br
kiony@yahoo.com.br
thamy.hayashi@mecanica.ufrgs.br
andresmendiburu@ufrgs.br

Abstract. *Research into alternative fuels is essential to ensure the energy sustainability of their practical application. Recently, there has been interest in fuels containing hydrogen, natural gas, biomethane and their blends. It is essential to study the flame propagation behavior of the alternative fuels in order to take proper safety measures for their use. A premixed flame propagating in a duct has several characteristics of the flame mixture, such as its acceleration in the early stages of propagation. The acceleration of the flame is important because under certain conditions deflagration can turn into detonation, which is a major hazard for practical applications. The objective of the present work is to characterize the flame acceleration of premixed flames propagating in closed channels. Therefore, experiments were performed to measure the propagation speed of the flame and to observe the acceleration of this flame. Characterizing the flame acceleration of alternative fuels is not an easy task given the wide variety of mixtures that can be realized. Therefore, in the present work, the mixtures are classified according to their Lewis and Zeldovich numbers. In this way, the authors attempt to make general observations applicable to alternative fuels with similar Lewis and Zeldovich numbers. In this study, the correlation of acceleration with Zeldovich number and effective Lewis number was analyzed. The mixtures were prepared with different concentrations of natural gas, hydrogen, and helium and were selected based on their effective Lewis number. The Lewis numbers of the mixtures ranged from 0.609 to 1.364 and the Zeldovich numbers ranged from 4.249 to 8.458. In addition, the tests were performed without any obstructions in the channel and then the same mixtures were tested in the channel with two orifice obstructions near the ignition end, which had a blocking ratio of 0.75. All experiments were conducted at an initial pressure of 40 kPa, an initial temperature of 313 K, and an equivalence ratio of 1.0.*

Keywords: *flame acceleration, Lewis number, Zeldovich number.*

1. INTRODUCTION

Given the increasing demand for energy and the goal of reducing greenhouse gasses, the study of alternative fuels is interesting and fundamental to ensure the sustainability of energy supply in practice. Recently, there have been studies on natural gas, hydrogen, biomethane and their blends. These fuels are used in internal combustion engines and gas turbines (Verhelst et al., 2009). For a premixed flame propagating in a duct, there are several features to be analyzed, such as the acceleration of the flame in the early stages of propagation. Flame acceleration is important because under certain conditions deflagration can transition to detonation. When this transition occurs in gas mixtures, it poses a great danger for practical applications, since the pressure increase can reach about 20 times the initial pressure. From this perspective, it is necessary to study the behavior of flame propagation in order to take the right safety measures when using alternative fuels to make the most of these new energy sources.

In recent years, much research has been done on the combustion of premixed gasses, analyzing the behavior of the flame wave in an obstruction-free closed channel. These studies are mainly concerned with the variation of parameters such as fuel composition and equivalence ratio, and the effects on the properties of the premixed flame that directly affect its propagation.

Thus, when a flame propagates in a tube or duct, the geometry of the flame front is a fundamental parameter in the initial phase of flame propagation. The flame propagates in an elongated shape (finger flame) and its velocity increases exponentially with time (Bychkov et al., 2007). However, at the moment when the flame touches the walls of the channel, the propagation speed decreases significantly (Valiev et al., 2012). During the detailed study of the basic characteristics of flames in closed channels, it was found that the flame acceleration is directly related to the turbulence caused by friction on the channel walls (Ciccarelli and Dorofeev, 2008). Later, it was proved that the characterization of the flame behavior is obtained from basic parameters such as the velocity of the laminar flame and the ratio between the density of unburned and burned gases (Dorofeev, 2011). In addition, the flame acceleration is affected by the instability depending on the turbulence, the presence of obstacles and confinement, and there are peculiarities in the initial and boundary conditions of the problem (Dorofeev, 2011).

Numerical and experimental analysis in the initial stages of flame (deflagration) demonstrated that for stoichiometric hydrogen-oxygen mixtures there is an effect of Mach number on flame acceleration, with the growth rate of flame acceleration decreasing with increasing Mach number (Valiev et al., 2012).

In a recent experiment (Zheng et al., 2016) in an obstacle-free closed glass duct defined that propagation speeds in all tests increase considerably with increasing hydrogen fraction, using five stoichiometric mixtures of hydrogen, methane, and air with different volume fractions of hydrogen (from 0% to 100%) and different aspect ratios (AR), it was found that the propagation velocities in all tests increase significantly with increasing hydrogen fraction.

In order to investigate the flame propagation velocity relationship for different compositions, experiments were conducted with premixed flames in a closed duct with a natural gas-air mixture with different equivalence ratios (φ) ranging from 0.67 to 1.50, a methane-air mixture with φ ranging from 0.61 to 1.36, and an acetylene-air mixture with φ ranging from 0.40 to 1.70 (Jin et al., 2017). The fuel composition was found to have an effect on the flame speed, as the natural gas-air mixture had a higher propagation speed than the methane-air mixture due to the low ethane and propane concentrations in the natural gas. However, when comparing the three mixtures, acetylene had the highest velocity due to the higher chemical reactivity of alkynes.

An experiment conducted by Mendiburu et al. (2019) in a closed channel to analyze the formation of tulip flames in ethanol-air mixtures shows that the flame propagation velocity is about 70 times the laminar flame velocity and this velocity is reached at a distance of about 9 times the channel radius. The experiments were carried out in a channel with a circular cross-section of 9.7 cm in diameter and 150 cm in length with φ from 0.90 to 1.40, the initial pressures from 20 to 60 kPa and initial temperatures of 32 ± 2 °C.

In addition to studies in closed ducts without obstructions, studies in closed ducts with obstructions are performed to analyze the effects of reducing the cross section on the propagation velocity of premixed flames. A theoretical and computationally proven study shows that in ducts with obstacles, the tip of the flame propagating in the unobstructed part of the duct leaves pockets of unburned fuel mixture between the obstacles, resulting in delayed combustion between the obstacles (Valiev et al., 2010). This late combustion is associated with various levels of turbulence created by the displacement of the flame. According to Valiev et al. (2010), when the distance between obstacles is large (ratio between distance and radius equal to 2), the velocity of the flame tip in each obstacle increases, and strong turbulent pulsations are observed, with the maximum velocity of each pulse equal to about half the distance between two obstacles. The formation of vortices downstream of each obstacle has already been observed by Johansen (2009) using the Schileren technique.

To visualize flame acceleration in a square channel with obstacles, an experimental study was performed in three cases with stoichiometric mixtures of hydrogen and oxygen with different numbers of obstacles with height and thickness of 0.0190 m and 0.0127 m, respectively (Boeck et al., 2016). The Schileren technique and planar laser-induced fluorescence (PLIF) helped in the observation. In the first case, one obstacle within the 0.495 m channel and an initial pressure of 25 kPa were used. In the second case, three obstacles within the 0.610 m channel and an initial pressure of 25 kPa were used. Finally, in the third case, eleven obstacles within the 1.220 m long channel and an initial pressure of 12.5 kPa were considered. According to Boeck et al. (2016), flame turbulence results from interactions between the flame and the shock waves and not from interactions with vortices formed at the edges of the obstacles.

A recent experimental work (Li et al., 2021) studied the propagation of methane-air flames with different mixtures in a closed channel with obstacles. Different volumetric concentrations of methane were used: fuel-lean (φ= 0.8), stoichiometric (φ= 1.0), and fuel-rich (φ= 1.2). In addition, methane was mixed with carbon monoxide, hydrogen, ethylene, and ethane, with the volumetric fraction varying from 0% to 2%. The barrier with a barrier ratio (BR, the ratio between the barrier area of the barrier and the cross-sectional area of the vessel) of 18% was installed on the side opposite to the ignition. Moreover, according to Li et al. (2021), the stoichiometric mixture of methane and 2% hydrogen exhibited the highest dispersion velocity, confirming previous work such as Zheng et al. (2016). In addition, the obstacles caused a pause in the growth of the pressure curve (Li et al., 2021).

Based on the literature review, it can be determined that none of the aforementioned papers used dimensionless numbers as parameters for flame acceleration analysis. With this in mind, the objective of the present work is to

perform experiments on five mixtures with different Lewis numbers. First, the experiments were performed without obstacles in the channel and then the same mixtures were tested in the channel with two 0.75 BR aperture obstacles located near the ignition source. Based on the obtained data, the correlation of the acceleration of the premixed flame in different mixtures of natural gas (NG), hydrogen and helium in closed channels was studied as a function of the Zeldovich number (β) and the effective Lewis number (Le).

2. EXPERIMENTAL SETUP

The test bench consists of a spreading channel, a mixing chamber, a magnetic stirrer, pressure transducers, a vacuum pump, a NOVUS model data acquisition system, an ignition system, a control panel, valves, connectors and hoses. Polyurethane hoses with a diameter of 10 mm are connected to the cylinders for natural gas, synthetic air, hydrogen, helium and nitrogen, which are connected to the valves in the control panel. Through these valves you can control the supply of gasses to the mixing chamber and to the propagation channel.

Table 1 shows the mixtures studied in the present work. From the composition of each mixture and the equivalence ratio, the values of Le and Ze were determined, which depend, respectively, on the heat and mass diffusivity and depend on the values of the activation energy associated with the laminar flame speed (SL) and the adiabatic flame temperature, which were determined by chemical kinetic mechanisms, as shown in equation (1) and equation (2). These parameters used in the experiment were determined from the San Diego mechanism (available at https://www.ucsd.edu/) using Cantera software (available at https://cantera.org/). To vary the dimensionless parameters, helium was used as a diluent in mixtures of some fuels. In addition, the Zeldovich number ranged from 4.249 to 8.458 and the effective Lewis number from 0.609 to 1.364, as shown in Tab. 1.

The effective Lewis number and Zeldovich number are calculated from Eq. (1) and Eq. (2) and presented by Qiao et al. (2010) and Matalon et al. (2009), respectively.

$$Le = \frac{\alpha_{mix}}{D_{fuel-O_2}} \tag{1}$$

$$Ze = \frac{E_a (T_a - T_u)}{R T_a^2} \tag{2}$$

Where α_{mix} is the thermal diffusivity of the mixture [m^2/s], $D_{fuel\text{-}O2}$ is the mass diffusivity of the fuel relative to oxygen [m^2/s], E_a is the activation energy [J/mol], R is the universal constant of gases [J/(mol.K)], T_a is the adiabatic flame temperature [K] and T_u is the temperature of the unburned gases.

Table 1. The mixtures studied with their respective Zeldovich and Lewis numbers.

Reference	Mixture	Ze	Le
A	NG + air	8.202	1.097
B	NG + 10%He + air	8.458	1.364
C	15%NG + 85%H_2 + 30%He + air	4.457	0.991
D	15%NG + 85%H_2 + 20%He + air	4.249	0.812
E	50%NG + 50%H_2 + air	6.093	0.609

The experiment consists of a mixing chamber coupled to a magnetic stirrer, a vacuum pump, and a square stainless steel channel with a diameter of 100 mm. The channel consists of three modules with a length of 350 mm, for a total of 1050 mm, but only two of the three modules were used to check the deflagration part. The flame in the channel is observed through two displays made of borosilicate glass with a thickness of 25 mm and a length of 250 mm. The two orifices used as obstacles have an outer diameter of 100 mm and an inner diameter of 50 mm (BR = 0.75) and were placed near the spark plug at a distance of 150 mm and 50 mm, respectively. The ignition system consists of an NGK type R spark plug and a transformer that supplies a voltage of 8 kV and a current of 30 mA. The mixing chamber consists of a steel box with a length of 600 mm, a width of 600 mm and a height of 500 mm, which is combined with a glass display for viewing. Inside this box there is a balloon flask made of tempered glass with a capacity of 20 liters.

A Phantom Vision Research model v411 high-speed camera was used to capture the images with the following optical parameters: Aperture 1.8, 12000 frames per second and a resolution of 640 x 480. The acquisition of the videos captured by the camera was performed using the Phantom Camera Control (PCC) software. It is worth mentioning that the mixtures diluted with helium had to be treated with the tracker software available at https://physlets.org/tracker/ for better visualization.

Three pressure sensors were also installed along the bench: two along the duct and one at the mixing chamber. A 10 bar pressure sensor (TP -6875 Warme) was installed at the end of the duct, facing away from the spark plug, and a 1 bar pressure sensor (TP -6875 Warme) was installed at the top of the duct, 500 mm from the ignition source. Finally, a 2 bar sensor (RTP-420 jerk) was installed in the center of the upper surface of the mixing chamber. These data were monitored by connecting the pressure sensors to a FieldLogger brand NOVUS and thus connected to a computer. Figure 1 below summarizes the information about the experimental equipment.

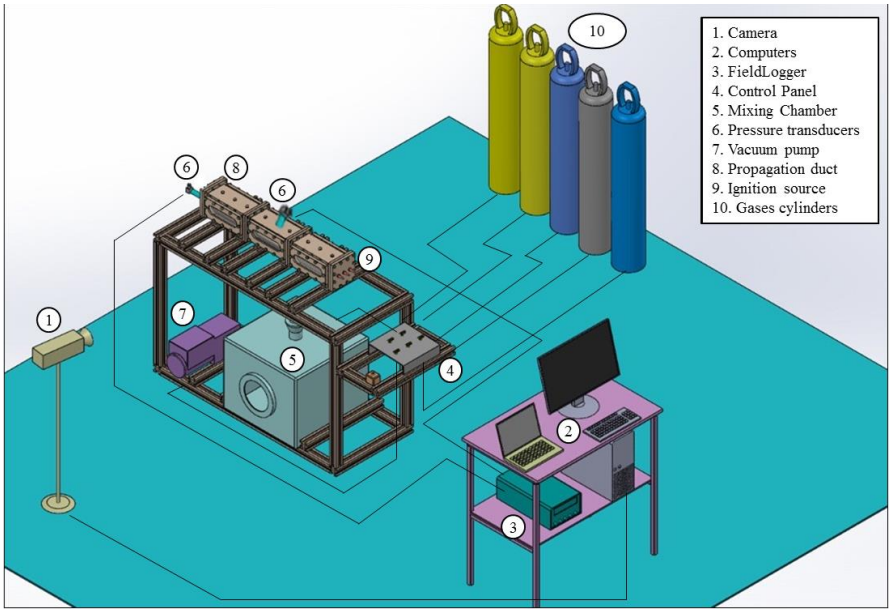

Figure 1. Experimental bench schematic. Adapted from Quines, (2022).

As shown in Fig. 2, the experimental procedure begins with evacuating the mixing chamber to a pressure of 0.5 kPa or less. Then, the gasses making up the mixtures were added using the partial pressure method: First, the natural gas was added to the chamber to the desired partial pressure, then the hydrogen and helium were added to their respective desired partial pressures, and finally the air was added until the final pressure was reached. The final pressure in the mixing chamber was 150 kPa. This pressure is sufficient to perform three repeated tests at 40 kPa in the propagation duct. The constituent gasses were mixed for 25 minutes, according to Mendiburu et al. (2018). After the entire mixing process, the duct was evacuated to a pressure of 0.5 kPa or less, and then the mixture was allowed to enter the duct up to a pressure of 40 kPa, triggering the ignition system, data acquisition system, and video recording system. For a new test, the duct is cleaned with nitrogen gas. Immediately after cleaning, the duct is evacuated again and the mixture contained in the chamber is returned to the duct at a pressure of 40 kPa and so on until the three tests are completed. After the three tests, the partial pressure method is repeated with the new mixture.

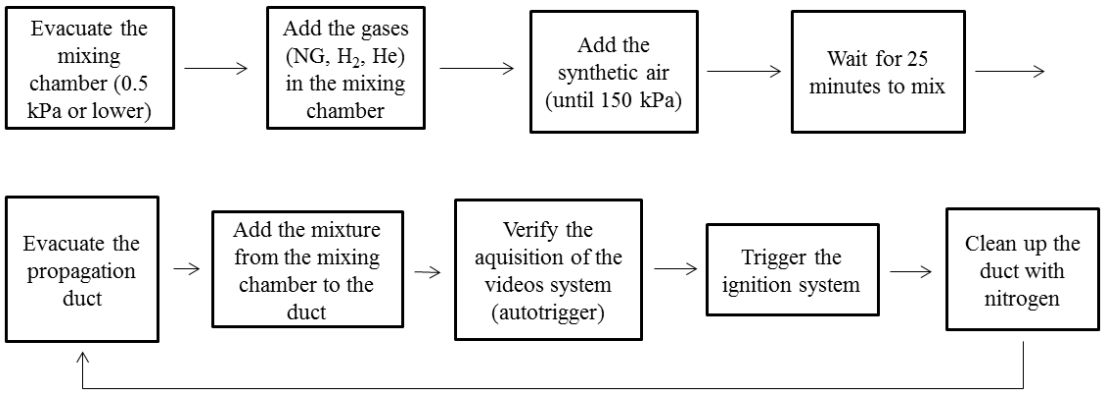

Figure 2. Experimental procedure diagram.

The flame propagation speed is determined by the tracker software from the range of distance and time of propagation of the flame front between images through a reference point. It is also worth noting that to determine the propagation speed along the duct, the values of the distance from the origin were considered, adding 4.5 cm to the experiments performed in the first window and 39.5 cm in the second window.

2.1 Associated Uncertainties

For the tests performed, the uncertainty was evaluated using the equivalence ratio of the mixture according to the method described by Holman (2011). The method is similar to a limiting case of the flammability of aviation kerosene (Rios Escalante et al., 2022). As shown in equation (3), an implicit function (R) is assumed to depend on the independent variables. According to equation (4), the magnitude of the total propagation of uncertainties depends on the uncertainty in the measurement of each independent variable. The partial derivative with respect to each variable is used to determine the total uncertainty by the product with the uncertainty with respect to the same variable.

$$R = f(x_1, x_2 ... x_n) \tag{3}$$

$$\omega_R = \left[\left(\frac{\partial R}{\partial x_1} \omega_1 \right)^2 + \left(\frac{\partial R}{\partial x_2} \omega_2 \right)^2 + ... + \left(\frac{\partial R}{\partial x_n} \omega_n \right)^2 \right]^{0.5} \tag{4}$$

The goal is to use the equation of the equivalence ratio to explain the parameters that directly affect flame behavior. The equivalence ratio is defined as the ratio between the number of oxygen moles in the stoichiometric state and the number of oxygen moles present in the mixture. For more complex mixtures with natural gas, hydrogen and helium, the number of oxygen moles depends on the mixing proportions of the individual fuels. For a defined mixture considering 1 mole of fuel, the value of the stoichiometric number of oxygen moles is constant. The number of oxygen moles (n_{O2}) is given in equation (5) and depends on the concentration of oxygen ($[O_2]$) and helium ([He]). The concentrations depend on the experimentally measured pressures for helium and oxygen, according to equations (6) and (7), respectively. Equation (8) shows the number of oxygen moles as a function of atmospheric pressure (p_{air}), helium pressure (p_{He}) and total pressure (p_{total}).

$$n_{O_2} = \frac{\frac{[O_2]}{100}}{1 - \frac{[He]}{100} - 4.76\frac{[O_2]}{100}} \tag{5}$$

$$[He] = 100 \times \frac{p_{He}}{p_{total}} \tag{6}$$

$$[O_2] = 100 \times \frac{0.21 p_{air}}{p_{total}} \tag{7}$$

$$n_{O_2} = \frac{0.21\frac{p_{air}}{p_{total}}}{1 - \frac{p_{He}}{p_{total}} - \frac{p_{air}}{p_{total}}} \tag{8}$$

Knowing the relationship between the number of moles and the pressure, you can define the relationship between the equivalence ratio and the pressures, as shown in equation (9).

$$\varphi = \frac{n_{O_{2S}} \left(1 - \frac{p_{He}}{p_{total}} - \frac{p_{air}}{p_{total}} \right)}{0.21\frac{p_{air}}{p_{total}}} \tag{9}$$

For the tests performed, the average for the observed equivalence ratio was 0.9993 with a standard deviation of 0.0248, i.e., at 95% confidence, the observed equivalence ratio is 0.9993 ± 0.049.

3. RESULTS AND DISCUSSIONS

Using the experimental data obtained under two conditions, the general behavior of the dispersion velocities and the influence of the fuel composition are first presented. Then, the relationships of the propagation velocities to the Zeldovich number and finally to the effective Lewis number are considered.

According to Fig. 3, Fig. 4 and Tab. 2, it can be seen that all the studied mixtures show the same behavior in the two proposed situations, namely an increase in the propagation velocity in window 1 and a slowdown in window 2. In cases without obstacles, all the mixtures, when analyzed dimensionless, show the same behavior, they are practically equivalent. However, in cases with obstacles, the mixtures show a tendency, but given the scatter of the data, it is only possible to state that the presence of obstacles increases the propagation velocities of the flame and increases the peak velocity by 3.1 to 5 times.

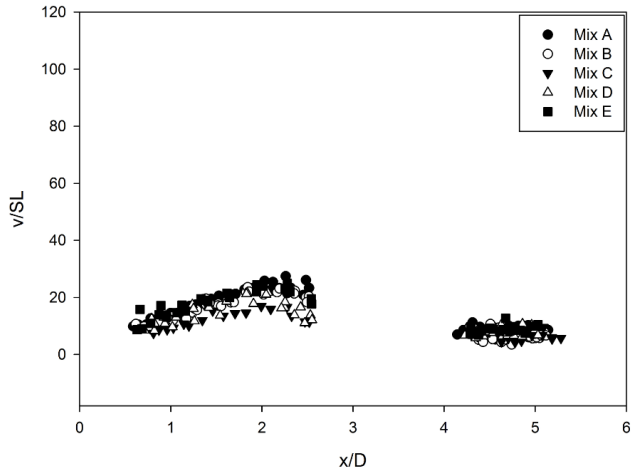

Figure 3. Dimensionless propagation speeds obstacles-free versus dimensionless distance.

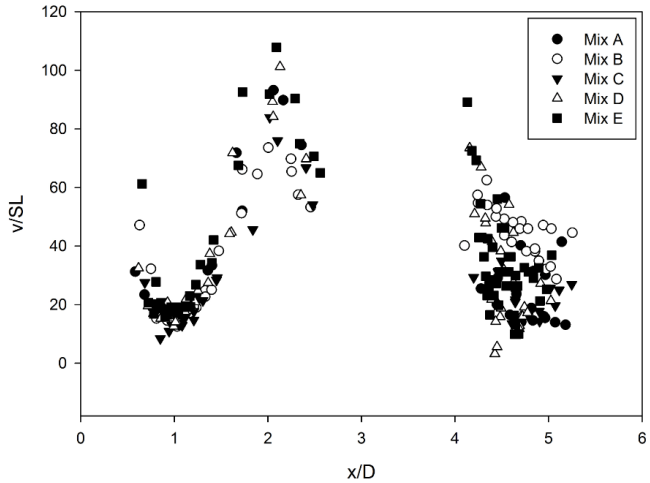

Figure 4. Dimensionless propagation speeds with obstacles versus dimensionless distance.

Figure 5 and Figure 6 show that the relationships between the maximum propagation velocities and the dimensionless numbers follow the same trend, with an upward shift in the graph when there are obstacles. In contrast, the relationships between the dimensionless propagation velocities do not follow the same tendency and change the order of the velocities in the two different situations, as shown in Fig. 5 and Fig. 6.

Table 2. The mixtures with their respective laminar flame, maximum dimensionless propagation and maximum propagation speeds with and without obstacles.

Mixture	Laminar flame speed [cm/s]	Dimensionless propagation speed obstacles-free	Dimensionless propagation speed with obstacles	Maximum propagation speed obstacles-free [cm/s]	Maximum propagation speed with obstacles [cm/s]
A	50.97	27.44	93.21	1398.53	4750.51
B	45.49	23.60	73.64	1073.48	3350.14
C	102.08	16.92	83.95	1726.70	8569.69
D	123.76	21.72	101.19	2687.68	12523.71
E	80.43	24.86	107.88	1999.60	8677.29

The mixture with the highest maximum speed is mixture D, whereas the lowest is mixture B, both in tests with and without obstacles. It is also seen that in the dimensionless analysis of flame acceleration without obstacles, mixture A has the highest propagation velocity and mixture C the lowest. On the other hand, in tests with obstacles, mixture E is the mixture with the highest propagation velocity and mixture B is the mixture with the lowest. This difference in the order of maximum spreading and dimensionless velocities for mixtures with helium can be explained by the difference between the laminar flame velocity predicted in the San Diego mechanism and reality. It is possible that this difference is due to the higher thermal diffusivity of helium, as this leads to a higher heat transfer rate with the channel, reducing the flame propagation velocity.

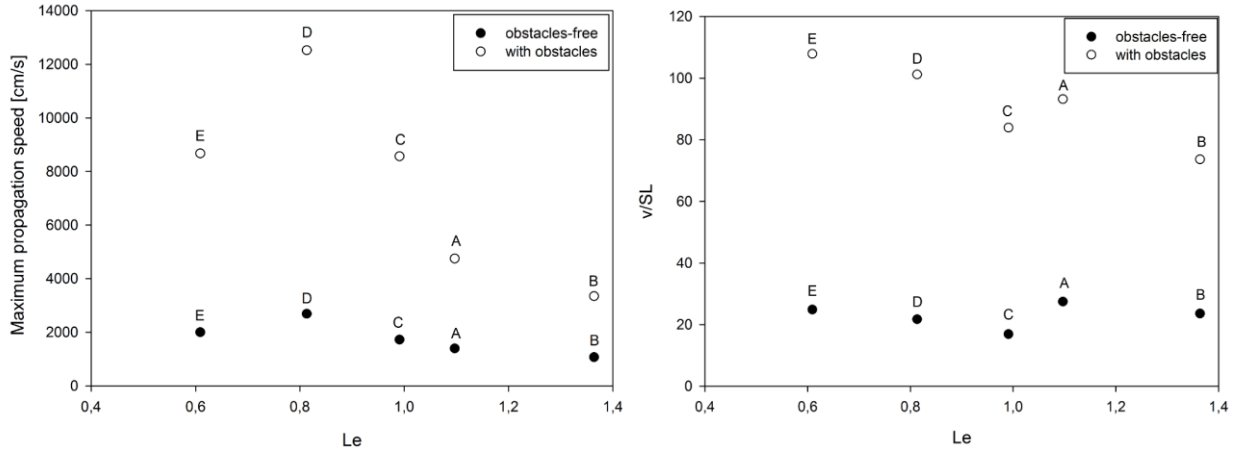

Figure 5. Maximum and dimensionless propagation speeds versus Lewis number, respectively.

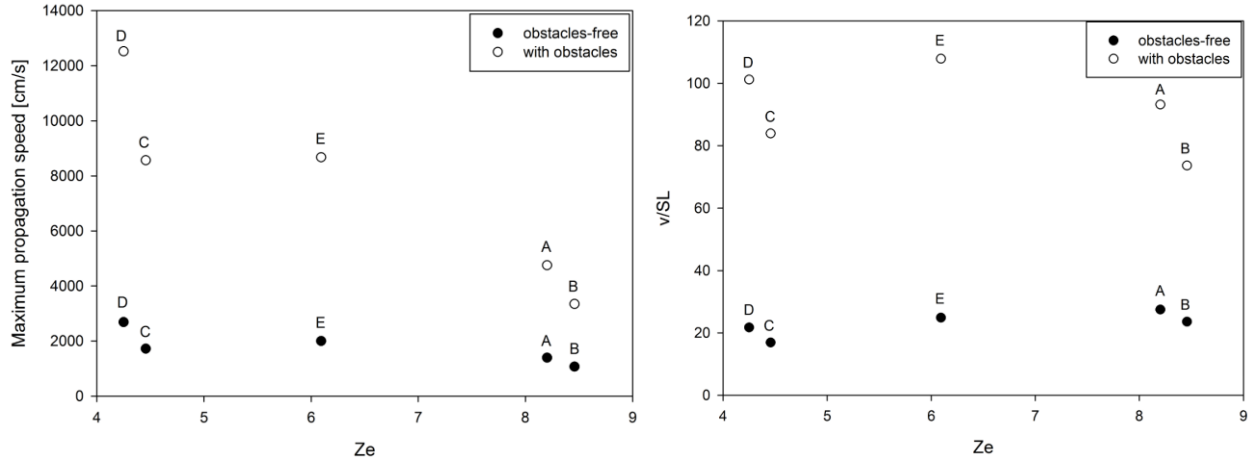

Figure 6. Maximum and dimensionless propagation speeds versus Zeldovich number, respectively.

The influence of fuel composition was analyzed and the flame propagation velocity increases when hydrogen is added, as shown by other authors such as Zheng et al. (2016) and Li et al. (2021). It is also shown that the propagation velocity decreases with increasing helium concentration when mixtures A are compared with B and D with C. In

mixtures with Le > 1, thermal diffusivity predominates, so heat diffuses easily from the flame to the walls, resulting in a temperature decrease in the flame. On the other hand, mass diffusivity predominates in mixtures with Le < 1, increasing flame propagation. This strength can be explained by the fact that the unburned gases move faster to the reaction zone.

In tests without obstacles, mixture B (Le= 1.364) is shown to have approximately the same velocity as mixture E (Le= 0.609), as previously shown by Alkhabbaz et al. (2019) for mixtures with Le= 0.5. In tests with obstacles, the propagation velocity of mixture E is higher and it still decelerates faster in window 2, as shown in Fig. 7. This slower acceleration in mixture B arises from the increase in flame front thickness due to the instability of the flame caused by the difference in thermal diffusion and mass diffusion.

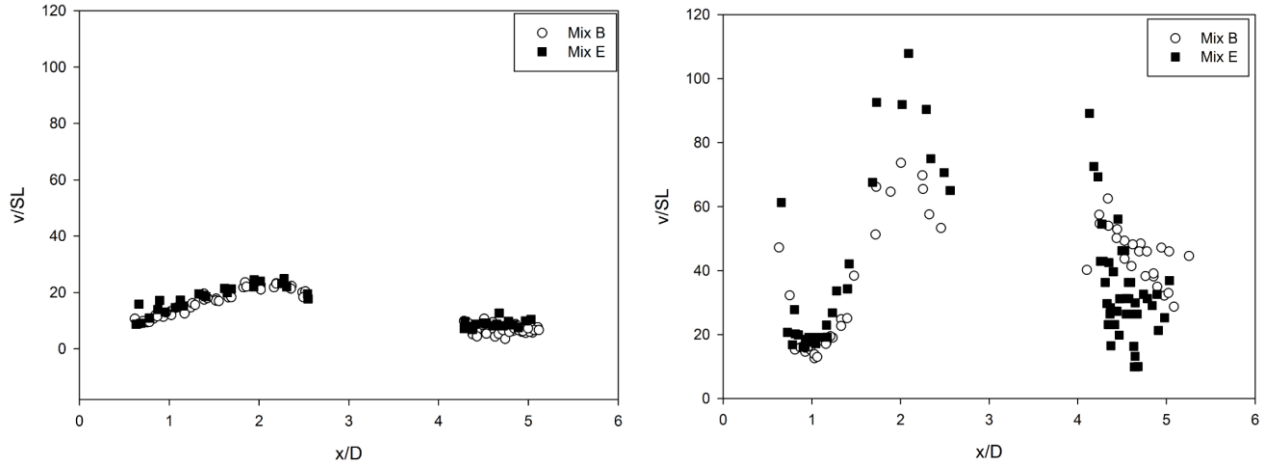

Figure 7. Dimensionless propagation speeds versus dimensionless distance without and with obstacles, respectively.

When comparing mixtures B (Ze= 8.458) and D (Ze= 4.249) in the tests with obstacles, the propagation velocity of mixture D is greater and the delay in window 2 is also greater, as can be seen in Fig. 8. On the other hand, for mixtures with similar Le and different Ze (mixture A and mixture C), the mixture with the highest Zeldovich number has a higher propagation velocity in both situations shown, as can be seen in Fig. 9. This unexpected result can be explained by the dilution of helium in mixture C, which acts like an inert in the reactions. The highest Zeldovich number is generally satisfied for reactions of interest for combustion and for combustion situations due to the higher activation energy and higher heat release from the chemical reaction in both cases (Law, 2006). The higher Zeldovich number implies a higher activation energy and a higher activation energy reflects the reactivity of the mixture, in other words, more energy must be provided to initiate and sustain the reaction of the reagents. In the case of a lower activation energy, it is easier to start a reaction. This explains the tendency for the activation energy to decrease with the increase of Ze, as shown in the first graph in Fig. 6.

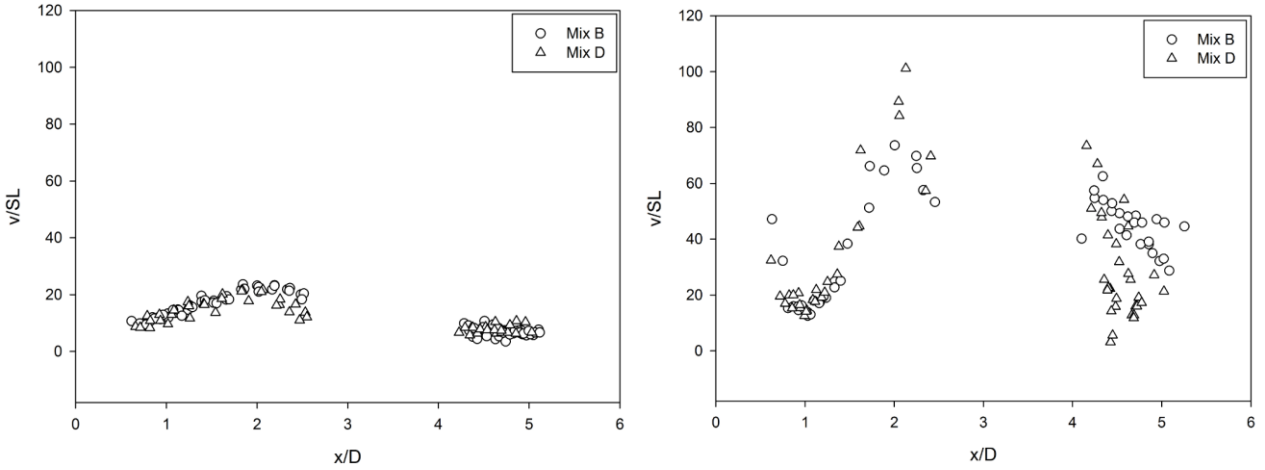

Figure 8. Dimensionless propagation speeds versus dimensionless distance without and with obstacles, respectively.

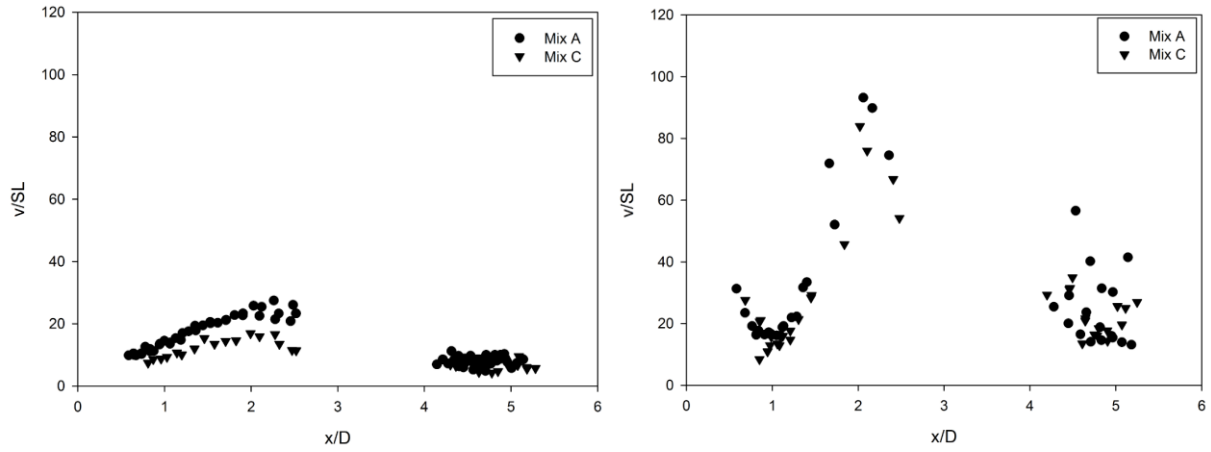

Figure 9. Dimensionless propagation speeds versus dimensionless distance without and with obstacles, respectively.

3.1 Empirical correlation

An empirical correlation was proposed to describe the maximum propagation velocity using the BR and the Zeldovich and Lewis numbers. An exponential model was chosen, depending on a pre-exponential and an exponential parameter, both with the dependence on BR as shown in Eq. 10. In addition, Tab. 3 shows the mixture with its respective product (Ze.Le) and the comparison of the calculated and measured maximum propagation velocities with their respective relative error. It is interesting to note that the relative error is less than 20%, which shows that the correlation is consistent with the experiments.

$$V_{\max} = \left(\frac{1}{1-BR}\right)^{1.25} 2988.9e^{\left((-0.088LeZe)\left(\frac{1}{1-BR}\right)^{0.34}\right)} \quad (10)$$

Table 3. The mixtures with their respective maximum propagation speeds (calculated and measured) and BR.

		BR = 0			BR= 0.75		
Mixture	Ze.Le	Vmax calc. [cm/s]	Vmax mes. [cm/s]	Relative error	Vmax calc. [cm/s]	Vmax mes. [cm/s]	Relative error
A	8.998	1354.07	1398.53	3,18%	4755.46	4750.51	-0.10%
B	11.537	1082.93	1073.48	-0,88%	3324.36	3350.14	0.77%
C	4.417	2026.32	1726.70	-17,35%	9071.82	8569.69	-5.86%
D	3.454	2205.41	2687.68	17,94%	10390.35	12523.71	17.03%
E	3.711	2156.25	1999.60	-7,83%	10021.71	8677.29	-15.49%

4. CONCLUSIONS

All the studied mixtures showed the characteristic behavior of flame front acceleration, starting with an acceleration ramp in the initial stages of propagation and later, in the final stages, a deceleration. The slowdown is directly related to the heat loss from the channel walls when flame propagation occurs. Mixture E has the highest propagation velocity and mixture B has the lowest when obstacles are present. Without the presence of obstacles, mixture A has the highest propagation velocity and mixture C the lowest.

In general, mixtures with lower Lewis numbers tend to be faster, but in some cases (Le near 0.6) mixtures with Le < 1 are comparable to mixtures with Le > 1 and achieve similar speed values. For mixtures with Le > 1, thermal diffusivity predominates, so heat diffuses easily from the flame to the walls, resulting in a temperature reduction in the flame. On the other hand, mass diffusivity predominates in mixtures with Le < 1, i.e. the unburned gasses move faster to the reaction zone.

The larger Ze represents a higher the activation energy, i.e., the mixture requires more energy to initiate and maintain the reaction of the reagents. At a lower activation energy, it is easier to start a reaction. Therefore, propagation rates tend to be faster at a lower Zeldovich number and slower at a higher Zeldovich number. The experiments show this tendency when analyzing the maximum propagation velocities, but when comparing the mixtures pairwise with the dimensionless velocity, it is not so consistent because the laminar flame velocity is different from the kinetic mechanism and reality.

In this regard, it is recommended to conduct more experiments on the dimensionless parameters and use different values of BR to check the correlation to improve the knowledge of the subject. Also, it is suggested to find another chemical kinetic mechanism with a larger capacity of reactions and an improvement of the speed acquisition system.

5. ACKNOWLEDGMENTS

The authors are grateful to CNPq (Conselho Nacional de Desenvolvimento Científico e Tecnológico) for supporting this work through Project 423369/2018-0 and to FAPERGS (*Fundação de Apoio à Pesquisa do Estado de Rio Grande do Sul)* for supporting this work through Project 21/2551-0000677-3.

6. REFERENCES

Alkhabbaz, M., Abidakun, O., Valiev, D., & Akkerman, V., 2019. Impact of the Lewis number on finger flame acceleration at the early stage of burning in channels and tubes. *Physics of Fluids*, *31*(8), 083606. https://doi.org/10.1063/1.5108805

Boeck, L. R., Kellenberger, M., Rainsford, G., & Ciccarelli, G., 2017. Simultaneous OH-PLIF and schlieren imaging of flame acceleration in an obstacle-laden channel. *Proceedings of the Combustion Institute*, *36*(2), 2807–2814. https://doi.org/10.1016/J.PROCI.2016.06.096

Bychkov, V., Valiev, D., & Eriksson, L. E., 2008. Physical mechanism of ultrafast flame acceleration. *Physical Review Letters*, *101*(16), 164501. https://doi.org/10.1103/PHYSREVLETT.101.164501/FIGURES/3/MEDIUM

Ciccarelli, G., & Dorofeev, S., 2008. Flame acceleration and transition to detonation in ducts. *Progress in Energy and Combustion Science*, *34*(4), 499–550. https://doi.org/10.1016/J.PECS.2007.11.002

Dorofeev, S. B., 2011. Flame acceleration and explosion safety applications. *Proceedings of the Combustion Institute*, *33*(2), 2161–2175. https://doi.org/10.1016/J.PROCI.2010.09.008

Holman, J. P., 2011. *Experimental Methods for Engineers*. McGraw-Hill Education. https://books.google.com.br/books?id=CZWFZwEACAAJ

Jin, K., Duan, Q., Liew, K. M., Peng, Z., Gong, L., & Sun, J., 2017. Experimental study on a comparison of typical premixed combustible gas-air flame propagation in a horizontal rectangular closed duct. *Journal of Hazardous Materials*, *327*, 116–126. https://doi.org/10.1016/J.JHAZMAT.2016.12.050

Johansen, C. T., & Ciccarelli, G., 2009. Visualization of the unburned gas flow field ahead of an accelerating flame in an obstructed square channel. *Combustion and Flame*, *156*(2), 405–416. https://doi.org/10.1016/J.COMBUSTFLAME.2008.07.010

Law, C. K., 2006. *Combustion Physics*. Cambridge University Press. https://doi.org/10.1017/CBO9780511754517

Li, R., Luo, Z., Cheng, F., Wang, T., Lin, H., & Liu, H. (2021). A comparative investigation of premixed flame propagating of combustible gases-methane mixtures across an obstructed closed tube. *Fuel*, *289*, 119766. https://doi.org/10.1016/J.FUEL.2020.119766

Mendiburu, A. Z., Serra, A. M., Andrade, J. C., Silva, L. M., Santos, J. C., & de Carvalho, J. A. (2019). Characterization of the flame front inversion of Ethanol–Air deflagrations inside A closed tube. *Energy*, *187*, 115932. https://doi.org/10.1016/J.ENERGY.2019.115932

Mendiburu Zevallos, A. A., Ciccarelli, G., & Carvalho Jr., J. A., 2018. DDT limits of ethanol–air in an obstacles-filled tube. *Combustion Science and Technology*, 1–16. https://doi.org/10.1080/00102202.2018.1477770

Quines R., 2022. *Estudo Experimental da Velocidade de Propagação de Chamas em um Duto Fechado*. Universidade Federal do Rio Grande do Sul, Porto Alegre, Brasil.

Rios Escalante, E. S., 2021. *Avaliação do Limite de Inflamabilidade Inferior e Concentração Limite de Oxigênio de misturas QAV – 1/etanol anidro em ar e atmosferas inertes*. Universidade Estadual Paulista "Júlio de Mesquita Filho", Guaratinguetá, Brasil.

Valiev, D., Bychkov, V., Akkerman, V., Law, C. K., & Eriksson, L. E., 2010. Flame acceleration in channels with obstacles in the deflagration-to-detonation transition. *Combustion and Flame*, *157*(5), 1012–1021. https://doi.org/10.1016/J.COMBUSTFLAME.2009.12.021

Valiev, D. M., Akkerman, V., Kuznetsov, M., Eriksson, L. E., Law, C. K., & Bychkov, V., 2013. Influence of gas compression on flame acceleration in the early stage of burning in tubes. *Combustion and Flame*, *160*(1), 97–111. https://doi.org/10.1016/J.COMBUSTFLAME.2012.09.002

Verhelst, S., & Wallner, T., 2009. Hydrogen-fueled internal combustion engines. *Progress in Energy and Combustion Science*, *35*(6), 490–527. https://doi.org/10.1016/J.PECS.2009.08.001

Zheng, K., Yu, M., Zheng, L., Wen, X., Chu, T., & Wang, L., 2017. Experimental study on premixed flame propagation of hydrogen/methane/air deflagration in closed ducts. *International Journal of Hydrogen Energy*, *42*(8), 5426–5438. https://doi.org/10.1016/J.IJHYDENE.2016.10.106

7. RESPONSIBILITY NOTICE

The authors are the only responsible for the printed material included in this paper.